Proceedings of the 17th World Congress
The International Federation of Automatic Control
Seoul, Korea, July 6-11, 2008

Rapid terminal area trajectory planning for reentry vehicles

Shuguang Zhang*, Peng Tang**

Department of Aeronautic Science and Engineering, Beihang University, Beijing, 100083, P.R. China
(* Tel: +86-10-82315237; e-mail: gnahz@buaa.edu.cn)
(** Tel:+ 86-10-82317703; e-mail: tangpeng@buaa.edu.cn)

Abstract: Achievements of the Space Shuttle experience and recent research activities were analyzed and absorbed, and a rapid generation technique of trajectories was focused on for the terminal area of reentry runway-landing flight vehicles. Based on the present processing capability of onboard computers, the trajectory geometry preset planning can be replaced by logic condition based algorithms which can represent the flight dynamics, so that the accuracy and rapidness can be better compromised. In view of the separation of the variation time scales, a propagation logic without iteration was established for longitudinal variables, combined with lateral effect correction. For the lateral motion, a three-step logic was put forward compromising the flexibility and effectiveness. Testing cases from different initial conditions show that the algorithm is promising for onboard application. It can rapidly generate trajectories with satisfactory accuracy due to the incorporation of the coupling effects in flight dynamics, and the guidance commands can be tracked by basic guidance control law.

1. INTRODUCTION

The unpowered terminal area flight of a reentry begins after the vehicle has entered the atmosphere and heating constraints are no longer a concern (nominally when velocity reaches Mach 2.5 or 3), or from a failure state soon after the launch, and ends when it enters the preset approach and landing interface (ALI, nominally at altitudes between 3km to 5km and Mach 0.5). For landing on a runway, the objectives of the reference trajectory is to bring the vehicle to an appropriate energy level landing, and align the vehicle heading with the runway.

The terminal area energy management (TAEM) technique of the Space Shuttle has proved to be effective and successful in view of the 1980s' computer memory storage and running capability level, and has been taken as classic for reentry runway-landing vehicles. The reference trajectory depends on well defined geometric segments, which are the S turn, the acquisition, the heading alignment cone (HAC), and the prefinal approach respectively, and the energy status is judged according to the preset offline generated energy vs. range-to-fly corridor (Moore, 1991). The lateral and longitudinal guidance channels are independent.

The need for reusable launch vehicles (RLV) stimulates the development of the TAEM methodologies, which pay more emphasis on the tolerance to unexpected initial errors, the capability of onboard trajectory generation, the disposal ability to failures, as well as on the accuracy and robustness of the algorithm (da Costa, 2003; Grubler, 2001; Hull *et al*., 2005; Kluever *et al*., 2005; Schierman *et al*., 2004). Many of the recent achievements are based on the Space Shuttle's TAEM algorithm, *e.g.*, replacing the two fixed HAC locations with a continuously adjustable location to permit a wider initial conditions (Kluever, 2005); using a spiral model in stead of the circular model in the estimation of the range-to-fly in the acquisition phase to be more accurate (da Costa, 2003), and so on. The improvements are helpful, but while they can keep the successful points of the Space Shuttle's TAEM algorithm, they will inevitably inherit the basic limitation of the algorithm based on the 1980s' computer memory storage and running capability level.

To clear the above bottleneck problems, the basic dynamics need to be reviewed, and some novel TAEM strategies have to be put forward. Along this way, a MIT research team has made achievements (Grubler, 2001). In stead of the decoupling of the longitudinal and the lateral reference trajectories as in the Space Shuttle's TAEM, the three degree of freedom mass-point dynamic equations are used to generate the flight trajectory as guidance reference. The errors due to the assumption of decoupling among axes and the estimation of range-to-fly can hence be removed, and more failure modes are potentially tolerable, but new challenges emerge, among which the effectiveness of the numerical algorithm is of first importance, or some simplification process is still in need.

Taking in some basics of Grubler's algorithm in this paper, a modified numerical iterative logic has been formatted for the algorithm to run more efficiently, and a more flexible maneuvering model has been used for the algorithm to be more adaptive.

2. DYNAMICS FORMULATION

In the TAEM phase with the Mach number dropping below 3, the flat earth model is accurate enough (Etkin, 1972), and the zero-sideslip and no-wind assumptions are reasonable for generating guidance reference trajectories. The three degree-of-freedom mass-point dynamics are expressed as in (1).

$$\begin{cases} \dot{V} = \dfrac{g}{W}\left(-D - W\sin\gamma\right) \\ \dot{\gamma} = \dfrac{g}{WV}\left(L\cos\mu - W\cos\gamma\right) \\ \dot{\chi} = \dfrac{g}{WV}\dfrac{L\sin\mu}{\cos\gamma} \end{cases} \tag{1}$$

Where, γ, μ, χ are the flight path angle, the roll angle and the heading angle respectively; L, D are the lift and the drag; and ρ, g, V, S, W are the air density, the acceleration of gravity, the flight velocity, the wing area and the weight.

For convenience of the TAEM application, the equations in (1) are reformed. In the unpowered TAEM flight phase, the altitude is monotonically decreased, and hence, this potential-energy representing variable can be used as alternative independent variable of the flight process. Another substitution is using the dynamic pressure for the flight velocity, in view that the dynamic pressure varies much slower than the velocity (the air density increasing and the flight velocity tending to decrease with the flight altitude descending), and hence, it becomes a more robust variable; moreover, that such dynamic constraints on the vehicle flight as the structural limitation and the ALI target conditions are expressed in terms of the dynamic pressure. Thus, the equations are transformed as in (2).

$$\begin{cases} q = \dfrac{W\cos\gamma}{SC_L\cos\mu - \dfrac{2W\sin\gamma}{\rho g}\left(\dfrac{d\gamma}{dh}\right)} \\ \dfrac{dq}{dh} = \left(\dfrac{1}{\rho}\dfrac{d\rho}{dh} - \dfrac{\rho g SC_D}{W\sin\gamma}\right)q - \rho g \\ \mu = \sin^{-1}\left[\dfrac{W\sin 2\gamma}{\rho g SC_L}\left(\dfrac{d\chi}{dh}\right)\right] \end{cases} \tag{2}$$

Where, C_L, C_D are the coefficients of lift and drag, and q is the dynamic pressure. The first equation represents the variation of the vertical trajectory under the action of the lift and gravity components, the second one represents the variation of the kinetic energy or the dynamic pressure, and the third one represents the variation of the projection of the trajectory on the horizontal surface, or namely the ground track. Noticeably, the variation of the dynamic pressure is not directly influenced by the roll angle, and the heading angle not directly influenced by the dynamic pressure.

3. THE TAEM STRATEGY

For the TAEM, the feasible flight state (in terms of q, γ, χ or other variables) vs. the independent variable process and the accompanying inner-loop commands (*e.g.*, commands of the angle of attack/normal load factor, the roll angle μ, and the speed brake deflection) should be determined according to the initial TAEM conditions (normal or failure entry), the ALI target conditions, the state constraints (the dynamic pressure constraint and others) and the inner loop command permission. From the viewpoint of mathematics, such trajectory generation problems can be formulated as the two point boundary value problems (TPBVP) with fixed starting and ending points and an optimal index, being numerically solvable. But, an efficient solution finding process requires that the trajectory space be bound, at designer's discretion. So a TAEM strategy follows.

In the Space Shuttle TAEM, the whole flight process is divided into four different segments of function. The initial segments are mainly to control the overall energy according the preset energy profile and the approach conditions, dissipating the redundant energy by S turns, while the later segments are mainly to adjust the geometry for approach and landing by winding the HAC. The definition of functions brings in simplicity and success, but as mentioned before there exist the innate flaws of accuracy limitation and inflexibility. (Moore, 1991)

Grubler and his team also started from a preset dynamic pressure profile, similar to the energy profile but dependant on the altitude instead of the range-to-go. A group of constant roll angles were then introduced to numerically solve the required flight path angles and angles of attack. After that, the heading angle, the roll angle and the ground track were determined by solving the two dimensional TPBVP according to the initial and the ALI requirements. Also a TPBVP solution needed, but a 2-dim case is much easier to deal with than a 3-dim case. To speed up the solution finding process, shaping of the ground track (the laterally maneuvering pattern) may be helpful, but carefulness is in need to avoid narrowing the trajectory solution space. Due to keeping the basics of the 3-dim mass-point dynamics while avoiding the direct TPBVP solution, the step by step process tends to give solutions of higher accuracy and more adaptability than those from the algorithm used in the Space Shuttle.

From the above reference trajectory solving process, the achieved probability of success, rapidness and precision depend on several key elements as the dynamic pressure schedule, the shaping of the lateral maneuvers, and the propagation logic for the longitudinal and the ground track.

4. GENERATION OF THE REFERENCE TRAJECTORY

4.1 Scheduling the Dynamic Pressure

In term of altitude, the dynamic pressure schedule is equivalent to the assigned energy profile, aligned with the description of motion dynamics, and can avoid the error due to inaccuracy of the range-to-fly estimation. The scheduling is based on the maneuverability of the vehicle and the requirement on the ground track length.

A multi-segment schedule may be useful, but for unmanned vehicles a three segment schedule is simple and working well in most cases. Three dynamic pressures are hence key, which correspond to the initial TAEM window, the desired steady state, and the ALI window (Fig.1). With the initial and terminal states determined, the scheduling is only the

definition of the steady state and the transition of the three pressure states.

Generally speaking, a higher dynamic pressure flight means a steeper flight path and shorter ground track, that gives adjustable margins for real ground track length cases. In addition, at higher dynamic pressures the lateral maneuverability will be further limited.

Across the transonic drag divergence region, a steady dynamic pressure flight will result in sinking of the flight path. If undesirable, the schedule should be modified and a lower dynamic pressure setting across the transonic region should help. For unmanned vehicles the sinking can often be left there for simplicity.

Moreover, the transition of the pressure states should be kept as smooth as possible for a smooth flight.

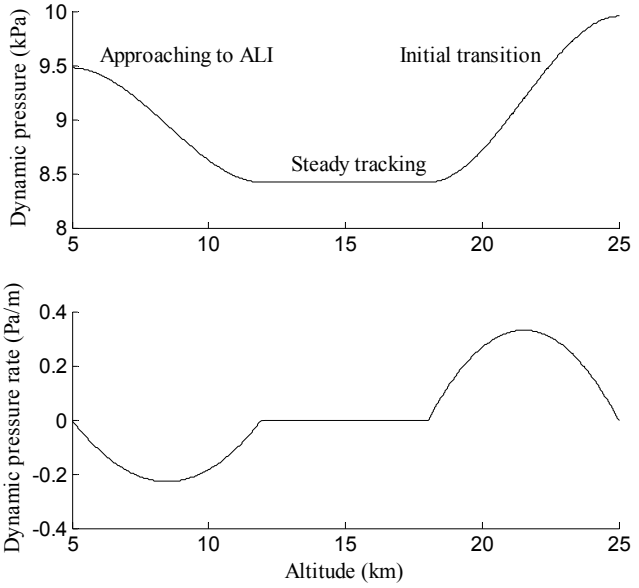

Fig.1. Dynamic pressure schedule

4.2 Shaping the Lateral Maneuvers

The complexity to solve the 2-dim TPBVP for the ground track can be cut down if the lateral maneuvering pattern is appropriate defined in view of the altitude dependent turning capability and the constraints on the ALI location and orientation.

In the paper, the lateral maneuvering pattern is basically defined as the rapidest successive turn, starting from the entry point of the TAEM phase, checked node by node, with three main segments to satisfy the requirements on the terminal heading angle, the crossrange and the downrange respectively. Without fixed geometry, the present lateral maneuvering pattern provides flexibility for various entry cases, the segment classification facilitates the solving, and the rapidest turning help achieve the terminal objectives quickly.

However, the rapidest turn may result in failures even if the flight requirements be achievable using other maneuvers. When the error in crossrange is large and the rapidest turn, with the maximal permitted normal load factor used, results in insufficient downrange, the trajectory generation fails. An option is to reschedule the desired dynamic pressure to a lower permitted value (modifying at outer solving loop), and another better option is firstly trying to decrease the used normal load factor and the roll angle (modifying at inner solving loop). Only when it is confirmed that the dynamic schedule does result in an extremely short ground track, a rescheduling follows.

4.3 Generating the Trajectory

The process of the trajectory generation includes the propagation of the longitudinal parameters and commands based on the scheduled dynamic pressure profile at given lateral maneuvering conditions, and the propagation of the lateral parameters, commands and the ground track at prescribed longitudinal parameters and the given lateral maneuvering pattern.

Firstly, the α and γ are solved by numerical propagation along the downward altitude according to the first two equations in (2), given the dynamic pressure and roll angle at each altitude node. If the altitude range is discretized into n-segments, and the state at the k-th altitude node is known, assuming that the α_k controlling $C_{D,k}$ and $C_{L,k}$ and hence the state at the (k+1)-th altitude node, so the propagation equations are in (3).

$$q_k = \frac{W\cos(\gamma_k)}{SC_L(\alpha_k, M_k)\cos(\mu_k) - \dfrac{2W\sin(\gamma_k)}{\rho_k g}\dfrac{\gamma_{k+1}-\gamma_k}{\Delta h}}$$

$$\delta q_k = \frac{q_{k+1}-q_k}{\Delta h} = \left[\frac{1}{\rho_k}\frac{\rho_{k+1}-\rho_k}{\Delta h} - \frac{\rho_k g SC_D(\alpha_k, M_k)}{W\sin(\gamma_k)}\right] q_k - \rho_k g \tag{3}$$

Solving α_k from the second equation, and γ_{k+1} from the first equation, all the solution can be propagated from the initial state to γ_n and α_{n-1} along the altitude nodes, where the α_k is taken as the cause of the motion (command of the inner control loop).

Naturally, the laterally solving step follows, and an iterative loop may be needed to update the roll angle used in (3) and the flight path angle and angle of attack in the third equation of (2) for lateral solution. However, iteration is time consuming. The technique used by Grubler is employed here to avoid iterating. According to the dynamic pressure schedule, the longitudinal command and state parameter lookup tables can be generated at a series of roll angles $\mu = [0,\mu_1,\ldots,\mu_n]$ (Fig.2). Due to good relevance of the state variable variation with the roll angle, the final solution of the longitudinal states can be determined by linear interpolation, rapid enough while resulting in negligible errors according to our application experience.

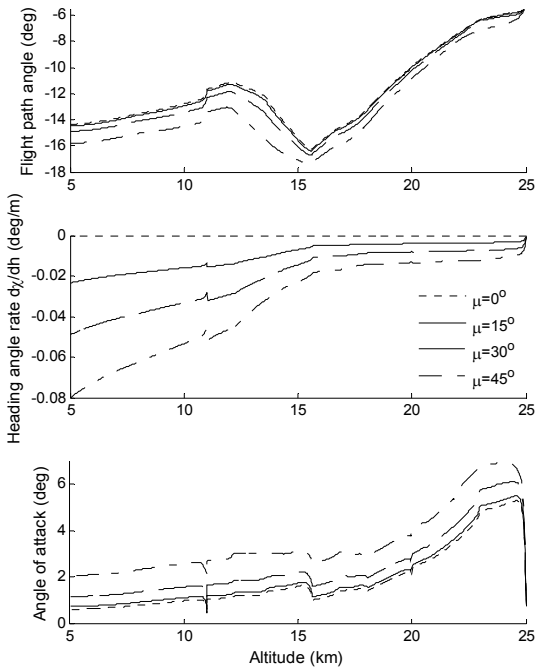

Fig. 2. γ, $d\chi/dh$, α schedules at different roll angles

The usable ground track is not necessarily unique and should meet all the constraints and terminate at the ALI positioning at the origin and aligning with the x axis in the present coordinate system. To find an appropriate solution, three successive steps are assigned to eliminate errors in the heading angle χ, the crossrange y and the downrange x (Fig.3).

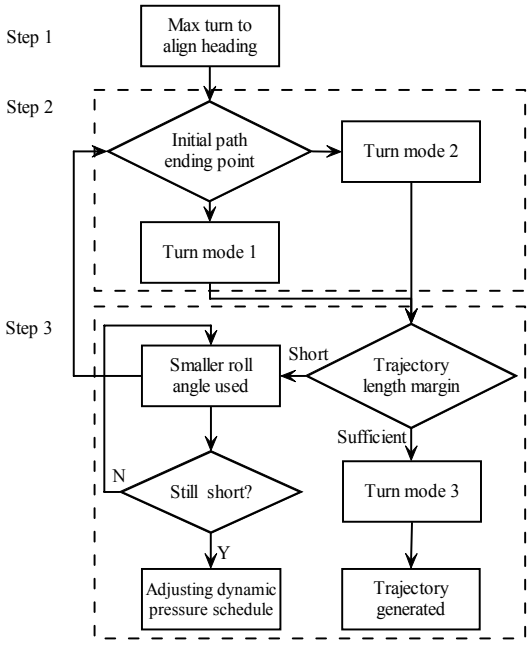

Fig. 3. Three step logic for ground track generation

Step 1, Turning to be aligned with the runway. Starting from the initial point of TAEM, the vehicle turns at the maximal capability limit by a node-to-node trial-and-error procedure, until its heading is aligned with the x axis. (Figs.4~6, the dotted lines)

Step 2, Turning to eliminate the error of crossrange y. Depending on the location of the vehicle with respect to the ALI after step 1, two turning modes are options. In the first turning mode the vehicle turns back to zero the crossrange in the opposite direction of step 1 (Fig.4, the dashed line), and in the second turning mode the vehicle keeps turning further along the same direction as in step 1 (Fig.5, the dashed line). Turning ends when the crossrange of the vehicle from the extension of the runway is zero, while in numerical solving the turning ends when two trajectories are generated which terminate at the opposite sides of the x axis, and the desired trajectory is taken out by interpolation.

Step 3, Turning or adjusting to eliminate the downrange error. After steps 1 and 2, two situations may appear. In the first situation, the trajectory terminates beyond the ALI, which means there is redundant energy to dissipate, and an additional turn follows (Figs. 4 and 5, solid lines). In the second situation, the trajectory terminates before achieving the ALI, which means there is energy shortage. To spare the energy, the trajectory is re-generated by to repeat steps 1 and 2 at a lower roll angle and lower normal load factor, until the ALI is achieved. If failed after the above solving loop, and the energy is innately short, then the dynamic pressure profile has to be modified to lower dynamic pressures, and a outer solving loop begins.

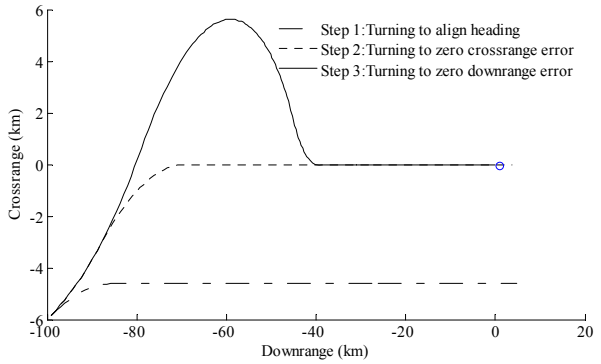

Fig. 4.Turning case 1

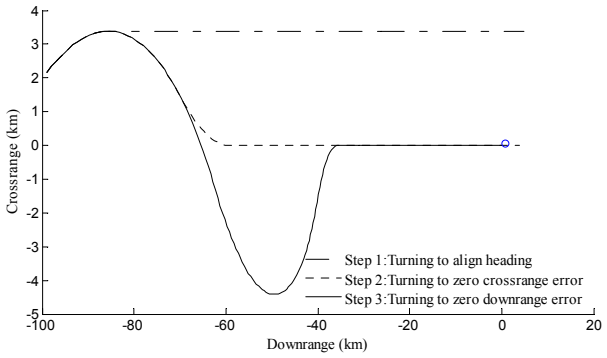

Fig. 5.Turning case 2

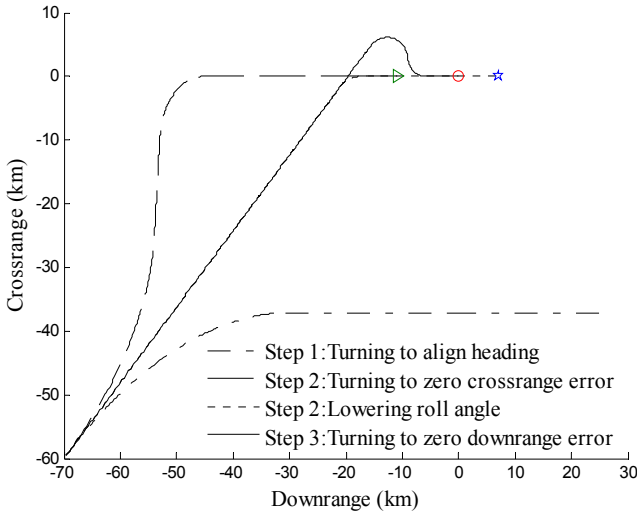

Fig. 6. Sparing energy by lowering the roll angle

5. TESTING CASES

Take the X-34 configuration (Pamadi, 2000) as the testbed. The initial TAEM state is set at altitude 25km and Mach number 2.5, while the ALI state is set at altitude 5km and Mach 0.5. The dynamic pressure is scheduled as in Fig.7. To establish the lookup table for longitudinal state variables and commands, the roll angles are set as in view of the maximum permitted roll angle of 45 degree:

$$\mu = [0, 15, 30, 35, 40, 45]$$

Besides the roll angle and the angle of attack, the speedbrake is also used as actuator in the subsonic region for guidance control.

Following the process stated in section 4.3, the trajectories for guidance reference have been generated, typical testing cases are as in Table 1 and the variable histories for testing case 1 as the dotted lines in Fig.7.

Table 1. Features of typical trajectories

Testing case No.	1	2	3	4	5
Initial downrange (km)	-100	-100	-70	30	15
Initial crossrange (km)	-6	2	-60	-50	30
Initial heading (deg)	10	10	50	180	-170
Turning mode	1	2	2	2	1
ALI downrange error (m)	3.1	10.2	-15.3	2.2	7.5
ALI crossrange error (m)	~0	~0	-7.7	-21.7	-16.3
ALI heading error (deg)	~0	~0	1.7	0.44	0.24
ALI dyn.pressure err.(Pa)	5	5	-98	14	21
ALI Mach error	<0.01				
Predicted flight time (s)	341	338	341	338	329
Max. normal load (g)	1.7	1.7	1.7	1.7	1.9

As in Table 1, for the preset typical testing cases the established trajectory generation algorithm can get reference trajectories with satisfactory accuracy and all constraints met. In view of the initial location and orientation cases 1 and 5 turn as in Fig.4, while cases 2, 3, and 4 turn as in Fig.5. For case 3, the quickest turn will result in shortage of energy, and hence a shallower and slower turn is used, and the reschedule of the dynamic pressure profile avoided.

To further verify the above results, three degree of freedom simulations have been run with a basic guidance law included, in which the heading is controlled by roll angle, the flight path angel controlled by angle of attack, and the dynamic pressure controlled by speedbrake if available in subsonic region, for testing case 1 as the dashed lines in Fig.7.

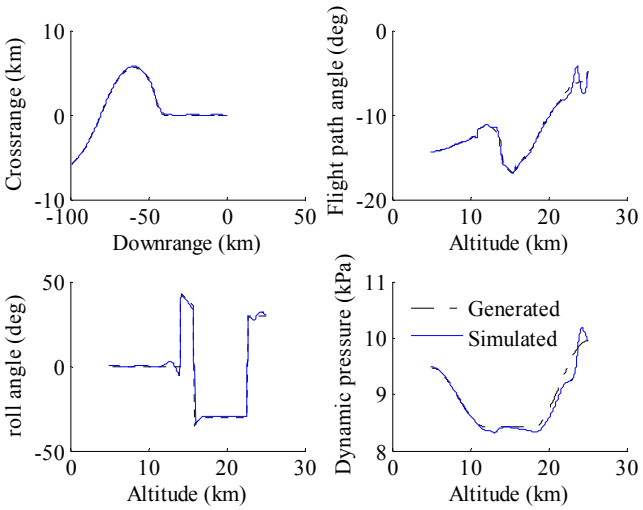

Fig. 7. Results of simulation

As Fig.7 shows, that the generated trajectory can be well tracked by the basic guidance law, and the inner loop commands are reasonable small, which means the established algorithm can incorporate the flight dynamics characteristics of the vehicle to generate the trajectories.

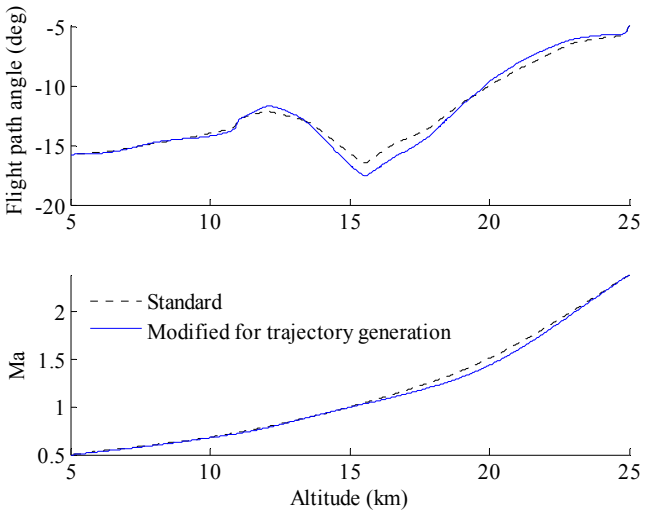

Fig. 8. Effect of the air density models on simulation

A point to pay attention is that due to the requirement on the smoothness of atmospheric model (derivative of the air density needed by eq.(3)), a modified nominal model has been used which is different from that used in the simulations, and a source of errors is then brought in. As in Fig.8 with different atmospheric models used, obvious errors can be observed, among which the error of the flight path angle tends to be the biggest than those of the Mach number and the heading.

The availability of onboard application of the algorithm depends on several key elements as: the capability of auto scheduling of the dynamic pressure, the rapidness of the generation of longitudinal lookup table at actual TAEM entry point, the rapidness of the ground track, the management of the solving process and the adaptability of the algorithm. About the rapidness, our testing experience shows that the ground track generation may be most time consuming.

Table 1 shows the needed computing time for the ground track generation of testing case 1 in the MATLAB© environment by the above stated three-step logic at different altitude intervals, and step 3 tends to be most time consuming. The needed time at a interval of 200m is negligibly short compared with the predicted flight time, but the generated trajectory is rough; on the contrary, the needed time at a interval of 50m is much longer, while the generate trajectory is satisfactorily accurate. Of course, as in an explanatory computer language environment, codes run very slow in MATLAB©, but it is not the case if converted into onboard codes, which means promising even at a dense altitude internal for accuracy consideration.

Table 2. Time consumed to generate ground track in MATLAB© environment

Altitude interval (m)	50	100	200
Time for step 1 (s)	0.1406	0.1250	0.1094
Time for step 2 (s)	1.2188	0.3594	0.1719
Time for step 3 (s)	37.7188	3.3281	0.7188
Total consumed time (s)	39.0782	3.6875	1.0001
Predicted flight time (s)	341		

6. CONCLUSIONS

1) The dynamic pressure scheduling is elementary and significant, because it determines energy dissipation requirement and the length of the ground track.

2) The propagation of the longitudinal states and commands is efficient and accurate enough if combining with the lookup table technique for consideration of the lateral coupling effect. Meanwhile, the effect of the air density model is noticeable.

3) The three step logic for ground track generation can eliminate the limitation of rigid geometry definition and provide flexible flight mode while run efficiently.

4) The established trajectory generation algorithm and process shows to be adaptive, accurate and promisingly rapid. However, comprehensive comparison and evaluation is needed for further on-board application.

ACKNOWLEDGEMENT

This research was supported by the 863 High Tech Project, and also the 111 Project of Ministry of Education and State Administration of Foreign Experts Affairs, P.R.China.

REFERENCES

da Costa, R.R. (2003). Studies for terminal area GNC of reusable launch vehicles. *AIAA-2003-5438*.

Etkin, B. (1972). *Dynamic of Flight-Stability and Control.* (2nd ed). John Wiley & Sons, Inc., New York.

Grubler, A.C. (2001). *New methodologies for onboard generation of terminal area energy management trajectories for autonomous reusable launch vehicles*. Thesis of MIT.

Hull, J.R., N. Gandhi, J. Schierman. (2005). In-flight TAEM/final approach trajectory generation for reusable launch vehicles. *AIAA-2005-7114.*

Kluever, C.A, K.R. Horneman. (2005). Terminal trajectory planning and optimaization for an unpowered reusable launch vehicle. *AIAA-2005-6058.*

Moore., T.E. (1991). Space shuttle entry terminal area energy management. *NASA TM 104744.*

Pamadi, B.N., G.J. Brauckmann, M.J. Ruth, H.D. Fuhrmann. (2000). Aerodynamic characteristics, database development and flight simulation of the X-34 vehicle. *AIAA-2000-0900.*

Schierman, J., D.G. Ward, J.R. Hull, N. Gandhi. (2004). Intelligent guidance and trajectory command systems for autonomous space vehicles. *AIAA-2004-6253.*